PHYSICAL REVIEW A VOLUME 38, NUMBER 7 OCTOBER 1, 1988

Near-threshold *K*-shell absorption cross section of argon: Relaxation and correlation effects

John W. Cooper
National Bureau of Standards, Gaithersburg, Maryland 20899
(Received 29 March 1988)

A detailed theoretical study has been made of the effects of core relaxation and electron-electron correlation on the near-threshold absorption cross section of argon, and the results are compared with previous calculations and experiment. The key results are the following: (1) Within the Hartree-Fock approximation, core relaxation must be included to obtain realistic cross sections; (2) final-state calculations are extremely sensitive to the way in which exchange effects are included in the calculations; (3) although electron-electron correlations produce only small changes in the single-electron cross section, they can account for the two-electron resonances which have been observed immediately above the ionization threshold. In particular, the main resonance above threshold appears to be $1s3p^53d^2$, which can be reached from the ground state via initial-state correlation.

I. INTRODUCTION

Although it is common knowledge that photoionization of deep atomic subshells is accompanied by the rearrangement of core electrons (the rearrangement leads to the emission of Auger electrons, additional electrons due to shake-off and shake-up processes and photons from core radiative processes) until recently little attention has been given to the effects of rearrangement on the photon absorption process. There are good reasons for this. At energies well above an inner-subshell threshold the absorption process is adequately described by single-electron central-field calculations[1] which yield absorption cross sections that agree with existing experimental data.[2] For energies above such thresholds, the physical picture of an electron being suddenly removed and no longer interacting with the ion core, followed by subsequent rearrangement leading to shake off, and radiative and Auger decay appears valid, and detailed calculations of the rates of these processes based on this formalism agree with existing experimental data.[3,4]

At near-threshold energies this simple picture is no longer valid and the effects of core relaxation and electron-electron correlation must be included in realistic calculations of photoionization cross sections. It is the purpose of this paper to examine these effects in some detail for a particular case, i.e., the photoionization of the *K* shell of atomic argon. This choice of a model system has been dictated by the following considerations.

(1) Recent experiments[5] have produced detailed experimental profiles of the near-threshold absorption cross section of argon which show dramatically the effects of electron correlation which result in two-electron excitation.

(2) Several attempts have been made recently[6-8] to account for relaxation in argon near-threshold *K*-shell photoionization. These efforts have led to a better understanding of the effects of core relaxation and provide the starting point for the work described here.

The remainder of this paper is structured as follows. Section II gives a survey of previous measurements and theoretical calculations. In Sec. III the basic theoretical framework of the work described here is discussed. Section IV contains the results of Hartree-Fock calculations of both the photoabsorption cross section and of the oscillator strengths of the autoionizing lines below the absorption threshold, and Sec. V presents the results obtained when configuration interaction is included. Finally, Sec. VI presents a summary of the results and suggestions for further theoretical and experimental work.

II. SURVEY OF EXPERIMENTAL AND THEORETICAL WORK

There have been a number of measurements of photoabsorption cross sections for argon in the energy range of the *K* ionization threshold. The earliest attempt to obtain a detailed profile of the *K* absorption edge was made by Parratt,[9] and similar results were obtained by Brogren.[10] This early work was followed by a more detailed study of the near-edge absorption by Schnopper[11] who obtained absolute values for the cross section and found evidence of two-electron excitation at energies of ~22 eV above the threshold. Similar results and evidence of additional two-electron excitation were obtained by Bonnelle and Wuilleumier.[12] The more recent work of Deslattes *et al.*[5,13] provides a much more detailed profile of the near-threshold cross section and shows that there are more resonances than the two previously found.

On the theoretical side of a number of calculations have been performed. As is shown in Ref. 5, a simple screened hydrogenic model with the screening adjusted to give the correct 1*s* binding energy agrees reasonably well with the most recent measurements except near threshold. Theoretical calculations using a relativistic central-field model[14] have recently been extrapolated to compare with the available experiments in the near-threshold region.[2] These results lie 14% below those of Ref. 5 in the near-threshold region but agree better with the earlier results.[11]

There have been three more recent calculations of the near-threshold cross section. Sukhorukov *et al.*[6] used the Hartree-Fock nonrelativistic dipole approximation to obtain results which agree rather well with the measurements of Ref. 11 provided the full effects of core relaxation are included. Amusia *et al.*[7] performed calculations using final-state wave functions generated in the potential of Ar^{2+} and also obtain good agreement with the results of Ref. 11. The most recent calculations are those of Tulkki and Aberg,[8] who performed several calculations using various models. Their results show that Dirac-Fock calculations including the effects of core relaxation reproduce the shape of the absorption cross section and lie about 8% below the results of Ref. 5.

III. THEORETICAL FRAMEWORK

A. Basic formulas

Excitation or ionization by a single photon of a K electron for a closed-shell atom such as argon can be described rather simply. If $\Phi_i(r_j)$ is taken to be the ground-state wave function of argon and $\Phi_f(r_j)$ the final-state wave function representing an atom with a single K-shell vacancy and one excited or free electron, the oscillator strength for discrete transitions and the differential oscillator strength/unit energy range for continuum transitions are given in dipole approximation by the well-known formulas:[15]

$$f=\tfrac{2}{3}(E_f-E_i)\,\Big|\sum_j \Phi(r_j)r_j\Phi_f(r_j)\Big|^2 , \tag{1}$$

$$df/dE=\tfrac{2}{3}(E_f-E_i)\,\Big|\sum_j \Phi_i(r_j)r_j\Phi_E(r_j)\Big|^2 , \tag{2}$$

where E_i (E_f) is the initial- (final-) state energy (in Ry), Φ_f represents a final discrete state, and Φ_E a continuum state normalized per unit energy. The photoionization cross section is given by

$$\sigma=8.067\times10^{-18}df/dE\ \mathrm{cm}^2 . \tag{3}$$

At this stage the following approximations have been made: (1) Use of first-order perturbation theory to derive the basic equations (1) and (2), (2) neglect of intershell coupling, (3) neglect of relativistic effects, (4) use of the dipole approximation.

Actually, approximations (3) and (4) need not be made. Relativistic effects and higher multipole excitation can easily be included if necessary. In the present case the errors made by these approximations are small and estimates of these effects will be given based on other calculations.

B. Wave functions

Equations (1)–(3) provide a prescription for the calculation of both the photoionization cross section and the oscillator strength of discrete excitations provided realistic wave functions for initial and final states are available. In the present work I have approximated initial- and final-state wave functions by Hartree-Fock methods. Basically, this is the same approach that was adopted in Refs. 6–8 and has been used previously in work on outer-shell photoionization,[16–18] and my work confirms and extends these previous results. In addition, the approach has the advantage that electron-electron interactions may be explicitly included using the Hartree-Fock results as a zeroth-order approximation.

C. The matrix element in the Hartree-Fock approximation

The starting point of the Hartree-Fock method is the representation of the initial- and final-state wave functions as the sum of Slater determinants of the form

$$\Phi_i(\underline{r}_i)=\frac{1}{N!^{1/2}}\det\Psi_{nlms}(\underline{r}_j) , \tag{4}$$

$$\Phi_{f,E}(r_j)=\frac{1}{N!^{1/2}}\det\underline{\Psi}_{fnlms}(\underline{r}_j) , \tag{5}$$

where

$$\Psi_{nlms}(r)=1/rP_{nl}(r)Y_{lm}(\theta,\phi)\sigma_s \tag{6}$$

and

$$\Psi_{flms}=1/r\underline{P}_{nl}(r)Y_{lm}(\theta,\phi)\sigma_s . \tag{7}$$

Here $P_{nl}(r)$ are radial orbitals, and $Y_{flm}(\theta,\phi)$ and σ_s the usual angular and spin functions for each orbital.

For a closed-shell atom, such as argon, the ${}^1S_0$ ground state may be represented as a single determinant and the derivation and solution of the nonrelativistic Hartree-Fock equations is a straightforward procedure.[19] The end result is a total energy E_t which is an upper bound to the nonrelativistic total energy and a set of radial orbitals $P_{nl}(r)$ which satisfy the orthogonality relations $\langle P_{nl}\mid P_{n'l'}\rangle=\delta_{nn'}$. Each radial orbital satisfies an equation of the form

$$P''_{nl}(r)+[Z_{nl}(r)-\varepsilon_{nl}]P_{nl} \\ =X_{nl}(r)P_{nl}(r)dr+\lambda_{nn'}P'_{nl}(1-\delta_{nn'}) . \tag{8}$$

For a closed-shell system as shown by Hartree,[20] the off-diagonal parameters need not be included in the radial equations. Here $Z_{nl}(r)$ is a central potential due to the charge distribution of the other electrons, ε_{nl} is the single-electron binding energy, $X_{nl}(r)$ is the nonlocal exchange potential, and $\lambda_{nn'}$ are Lagrange multipliers. Each orbital vanishes the $r\rightarrow0$ and has $n-l-1$ nodes.

For final states corresponding to a deep inner-shell hole and an excited or free electron, the procedure is not straightforward and a number of alternative approximations may be used to describe such final states. For excited discrete states, e.g., a $1s2s^22p^63s^23p^6np\ {}^1P_1$ excited state in argon, the procedure for deriving the Hartree-Fock equations for the radial orbitals is exactly the same as for closed-shell systems. However, in solving these equations certain constraints must be invoked in order to obtain realistic solutions, namely, the following.

(1) The one-electron eigenvalues ε_{nl} in Eq. (8) must correspond approximately to the binding energies of the electrons in the various subshells.

(2) In order to maintain orthogonality between orbitals, the off-diagonal parameters $\lambda_{nn'}$ in Eq. (8) must be included.

Constraint (1) is needed to maintain the required orbital occupancy. If it were neglected, solutions of the

Hartree-Fock equations would either fail to converge or converge to a state in which the initial vacancy has been transferred to an outer subshell. The second constraint requires more discussion. As shown previously,[21] the effect of including the off-diagonal parameters in the Hartree-Fock equations for inner-vacancy states is to introduce extra nodes in the radial wave functions obtained. If the off-diagonal parameters are neglected, the extra nodes are not present, and the total energy of the system is slightly lower than that obtained requiring orthogonality.

For continuum states yet another procedure must be used. If the wave function is to represent a free electron moving in the field of an ionic core in a specific state, the calculations must be done in two steps. First, a Hartree-Fock solution for the core orbitals must be found and then the radial equation for the continuum orbital corresponding to an electron in the presence of the core must be solved and normalized per unit energy range. For states involving inner-shell vacancies the first step is exactly the same as for excited discrete states, the only differences being the absence of a single electron in the orbital representation of the ionic state. Thus the same two constraints must be used to obtain realistic orthogonal orbitals. In the equation for the free-electron orbital, $P_{\varepsilon l}$ will be of the form of Eq. (8) with ε_{nl} replaced by the free energy and P_{nl} replaced by $P_{\varepsilon l}$. The above discussion has been given in some detail because, as we shall see in Sec. IV, the results obtained for inner-shell excitation and ionization are sensitive to how the exchange terms in Eq. (8) are estimated and how the orthogonality constraints are imposed.

Assuming that the initial and final states corresponding to the argon $^1S_0$ ground state and an excited or ionized state with an inner $1s$ vacancy corresponding to $^1P_1$ are represented as in Eqs. (4) and (5), it is a simple matter to evaluate the matrix elements of Eqs. (1) and (2).[22] For argon K-shell excitation the matrix element may be written as[6]

$$M = S(A - B - C - D - E)\,, \tag{9}$$

where

$$\begin{aligned}
S &= \langle P_{1s} \mid \underline{P}_{1s} \rangle \langle P_{2s} \mid \underline{P}_{2s} \rangle^2 \langle P_{2p} \mid \underline{P}_{2p} \rangle^6 \\
&\quad \times \langle P_{3s} \mid \underline{P}_{3s} \rangle^2 \langle P_{3p} \mid \underline{P}_{3p} \rangle^6 \,, \\
A &= \langle P_{1s} \mid r \mid \underline{P}_{\varepsilon p} \rangle \,, \\
B &= \langle P_{1s} \mid r \mid \underline{P}_{2p} \rangle \langle P_{2p} \mid \underline{P}_{\varepsilon p} \rangle / \langle P_{2p} \mid \underline{P}_{2p} \rangle \,, \\
C &= \langle P_{1s} \mid r \mid \underline{P}_{3p} \rangle \langle P_{3p} \mid \underline{P}_{\varepsilon p} \rangle / \langle P_{3p} \mid \underline{P}_{3p} \rangle \,, \\
D &= \langle P_{2s} \mid r \mid \underline{P}_{\varepsilon p} \rangle \langle P_{1s} \mid \underline{P}_{2s} \rangle / \langle P_{2s} \mid \underline{P}_{2s} \rangle \,, \\
E &= \langle P_{3s} \mid r \mid \underline{P}_{\varepsilon p} \rangle \langle P_{1s} \mid \underline{P}_{3d} \rangle / \langle P_{3s} \mid \underline{P}_{3s} \rangle \,.
\end{aligned} \tag{10}$$

Here $\underline{P}_{\varepsilon p}$ is the radial orbital for an excited or free electron, and only terms of first order in the overlap integrals for different n,ε are retained. Barred and unbarred orbitals indicate final and initial states, respectively.

Although Eq. (9) is not a new result it merits some discussion. First, note that the term S is the overlap factor used to compute the probability of two-electron excitation in the sudden approximation. The second term may be interpreted as the sum of probability amplitudes for direct excitation (A), of shake off induced by inner-shell transitions (B and C), and of dipole transitions from outer subshells induced by core relaxation (D and E).

At high energies the additional terms on the right-hand side of Eq. (9) vanish. In addition, since exchange effects become negligible, the orbital $\underline{P}_{\varepsilon p}$ represents an electron moving in the central field of the ion core. As discussed previously,[23] this leads to the interpretation of the cross section calculated using Eq. (9) as the single-electron cross section and $1 - |S|^2$ as the probability of double excitation due to core relaxation.

Basically the same formalism outlined above has been used previously in near-threshold computations of the photoionization cross sections for outer shells,[16–18] where core-relaxation effects were found to be negligible, and in the computation of radiative rates for inner-shell vacancy transitions,[24] where including the extra terms equivalent to those in Eq. (9) was found to result in an increase in the radiative rates.

IV. THE SINGLE-ELECTRON CROSS SECTION

Using the formalism developed in Sec. III, I have calculated the cross section for argon K-shell photoabsorption as well as the oscillator strength of $4p$ an $5p$ transitions. All calculations were performed using Cowan's set of atomic structure programs.[25] This set of programs includes two separate codes for performing Hartree-Fock calculations, the major difference between them being that for excited states the orthogonality of the core orbitals is strictly enforced in one version (O) and not in the the other (NO) and that strict orthogonality cannot be enforced for calculations involving a free electron. Since these differences are important in the present context, calculations using both versions were carried out.

A. Energy calculations

The total nonrelativistic energies obtained using both the O and NO versions for a number of calculations are given in Table I and compared with previous work. As expected, there is little difference (<0.001 Ry) in the total energy for the argon ground state between the present calculations and previous work. The same is not true for the $(1s)$ core-hole states of Ar$^+$ and the excited $(1s)/4p$ and $(1s)5p$ states, the NO calculations lying ~ 0.02 Ry lower in energy then the O calculations. Similar results were obtained by Bagus[21] who pointed out that these small energy differences would be expected to have a large effect on transition rates involving inner-shell electrons.

Both sets of calculations give good estimations of the $1s$ electron binding energy as shown in Table I. Note that there is less than 0.4% difference in the calculated binding energy from the experimental value.[26] Theoretical energies were used in all calculations.

B. Oscillator strengths for 4p and 5p transitions

Based on a careful analysis of the absorption cross sections of Ref. 11, Watanabe[28] obtained experimental oscil-

TABLE I. Hartree-Fock energies. c.g. denotes the center of gravity.

State			Present	Clementi[a] and Roetti	Bagus[b]	
Ar	S_0	O	1053.635 23	1053.634 78	1053.635	
		NO	1053.634 85			
Ar$^+$		O	818.778 33		818.778	
		NO	818.798 04		818.788	
Ar	$(1s)4p$	O, c.g.	818.969 50			
Ar	$(1s)4p$	NO, c.g.	818.989 21			
Ar	$(1s)4p$	O, ^{1}P	818.969 67		1s binding energy	
Ar	$(1s)4p$	NO, ^{1}P	818.988 36	O	NO	Expt.[c]
Ar	$(1s)4p$	O, ^{3}P	818.969 80	234.857	234.836	235.6
Ar	$(1s)4p$	NO, ^{3}P	818.989 50			
Ar	$(1s)5p$	O, c.g.	818.868 47			
Ar	$(1s)5p$	NO, c.g.	818.889 18			
Ar	$(1s)5p$	O, ^{1}P	818.869 18			
Ar	$(1s)5p$	NO, ^{1}P	818.889 89			
Ar	$(1s)4p$	O, ^{3}P	818.869 57			
Ar	$(1s)5p$	NO, ^{3}P	818.889 28			

[a]Reference 26.
[b]Reference 21.
[c]Reference 27.

lator strengths for the $4p$ and $5p$ transitions which appear as Auger broadened lines in the absorption spectrum immediately below the ionization threshold. Since previous work[6–8] has shown that calculations of this type are sensitive to exchange effects, we have calculated the oscillator strengths using several different methods whose results are compared with previous work in Table II.

There are two ways in which Hartree-Fock calculations can be performed for the final excited states. One can assume that the excited state corresponds to the center of gravity of the $1snp$ $^{1,3}P$ terms or alternatively perform separate ^1P and ^3P-term-dependent calculations. The only difference in the calculations is the coefficient of the exchange term for the np orbital [Eq. (8)]. The oscillator strengths calculated from both the term-dependent and center-of-gravity calculations show the extreme sensitivity of the calculation to exchange effects. The best agreement with the experimental values is the calculation done in the center-of-gravity approximation neglecting the orthogonality constraint. Note that the "best" calculation, i.e., the term-dependent calculation maintaining orthogonality, gives oscillator strengths ~30% below the experimental values and that the only calculation that shows reasonably good agreement with that of Ref. 6 is the term-dependent calculation ignoring the orthogonality constraint.

The major effect of exchange is to vary the amplitude of the np orbital at small distances as is shown in Table III. As expected, the larger the exchange term, the greater the amplitude of the np orbital near the nucleus.

Table IV lists all of the matrix elements and overlap integrals for the four alternative calculations of the $1s$-$4p$ matrix element. The table shows that most of the terms in Eq. (9) are insensitive to the method of calculation. The main difference between the O and NO results is due to the change in sign of the $(1s \mid \underline{2s})$ and $(1s \mid \underline{3s})$ overlap matrix elements which produce the major change in the total transition matrix element.

C. Photoionization cross sections

Near-threshold cross sections calculated using wave functions obtained via both the center-of-gravity and term-dependent ^1P calculations are shown in Table V and are compared with the experimental results of Ref. 5 in Fig. 1. In both Fig. 1 and in Table V total cross sections have been obtained by adding the extrapolated L- and M-shell contributions obtained from Ref. 14 to the calculated K-shell results. This contribution is 9.6×10^{-21} cm^2

TABLE II. Oscillator strengths (10^3) for $1s$-$4p$ and $1s$-$5p$ transitions.

	$1s$-$4p$	$1s$-$5p$
Hartree-Fock O, c.g.	1.61	0.517
Hartree-Fock NO, c.g.	2.01	0.662
Ref. 6	1.77	0.60
Expt (Ref. 27)	2.17±0.13	0.66±0.07
Hartree-Fock O, ^1P	1.47	0.475
Hartree-Fock NO, ^1P	1.84	0.594

TABLE III. Values of $P_{np}(0)/r$.

Calculation		$4p$	$5p$
O	c.g.	8.564	5.013
O	^1P	7.740	4.545
O	^3P	8.897	5.186
NO	c.g.	8.509	5.008
NO	^1P	8.130	4.780
NO	^3P	8.658	5.083

TABLE IV. Overlaps and dipole matrix elements for $1s$-$4p$ transitions.

Matrix element	O c.g.	O ^1P	NO c.g.	NO ^1P
$(1s\,\|\,\underline{1s})$	0.999 92	0.999 92	0.999 84	0.999 84
$(2s\,\|\,\underline{2s})$	0.998 81	0.998 81	0.998 78	0.998 78
$(3s\,\|\,\underline{3s})$	0.992 50	0.992 49	0.992 46	0.992 46
$(2pF\underline{2p})$	0.997 72	0.997 72	0.997 72	0.997 72
$(3p\,\|\,\underline{3p})$	0.983 56	0.983 50	0.983 54	0.983 52
$(1s\,\|\,\underline{2s})$[a]	0.001 67	0.001 68	−0.004 79	−0.004 78
$(1s\,\|\,\underline{3s})$[a]	0.000 49	0.000 49	−0.001 48	−0.001 48
$(2p\,\|\,\underline{4p})$	−0.004 98	−0.004 95	−0.004 98	−0.003 97
$(3p\,\|\,\underline{4p})$	−0.073 45	−0.073 07	−0.074 33	−0.070 20
$(1s\,\|\,r\,\|\,\underline{2p})$	0.065 36	0.065 36	0.065 23	0.065 26
$(1s\,\|\,r\,\|\,\underline{3p})$	0.016 36	0.016 36	0.016 40	0.016 40
$(1s\,\|\,r\,\|\,\underline{4p})$	0.002 21	0.002 06	0.002 21	0.002 20
$(2s\,\|\,r\,\|\,\underline{4p})$	0.016 86	0.016 15	0.017 08	0.016 46
$(3s\,\|\,r\,\|\,\underline{4p})$	0.149 74	0.147 60	0.149 23	0.141 82
S	0.8774	0.8772	0.8780	0.8771
A	0.002 21	0.002 06	0.002 21	0.002 20
B	0.000 33	0.000 33	0.000 33	0.000 26
C	0.001 22	0.001 22	0.001 24	0.001 17
D[a]	−0.000 02	−0.000 03	0.000 08	0.000 08
E[a]	−0.000 08	−0.000 07	0.000 22	0.000 21
M	0.003 20	0.003 07	0.003 58	0.003 43

[a] Indicates change of sign.

at threshold and agrees well with experimental results.[2] Both calculations give the same shape as the experimental results in the region immediately above the absorption threshold and lie within 5% of the experimental values. At higher energies the calculations lie below the experimental results and the difference can be attributed to two-electron excitation. Note that at 10 Ry above the threshold, the two calculations differ by less than 5%. All of the calculations shown were made using Hartree-Fock orbitals for the Ar II core which were not orthogonal. The good agreement of our ^1P results with the calculations of Ref. 8 seems to imply that the orthogonality between the core states was not maintained in their calculations.

Although photoionization cross sections have not been calculated using orthogonal core orbitals, we can anticipate the results. In Fig. 2 we show near-threshold values of df/dE computed from Eq. (2) and f values below threshold normalized per unit energy range, compared with the experimental data. The figure shows that an extrapolation of the discrete-state orthogonal results would yield cross sections at threshold considerably below the experimental results. I have not done calculations using the velocity form of the matrix element, but I have examined relativistic effects. The programs used estimate relativistic effects approximately by adding a small spin-orbit term to the central potential. Calculations made using this option increased the cross sections calculated slightly, but no more than 2%, in agreement with Ref. 8, which also shows that the dipole approximation is valid to approximately 1.0% for calculations of this type.

V. TWO-ELECTRON EXCITATION

Although many-body effects are present in the results of the previous section since exchange and core relaxation are included, the results still represent the excitation or ionization of a single K-shell electron. Note that in Fig. 1, while the calculations agree very well with the results at energies below 3220 eV, they show no resonance structure and lie below the experimental curve at higher energies. The resonances are, of course, due to two-electron processes, and estimates of these effects will be discussed below.

There are two ways in which two-electron excitation can occur when a deep inner-shell electron is ionized. First, as we have seen in Sec. IV, when inner-shell ionization occurs, the remaining orbitals are no longer orthogonal and dipole transitions in the core make a large contribution to the total matrix element for excitation. When a threshold for double excitation is reached, core-relaxation effects can induce transitions to doubly excited states. Cross sections for excitation due to this process can be calculated in the same way that the single-electron cross section is obtained including the effects of core relaxation.

Second, while the Hartree-Fock approximation provides an excellent description of the inner atomic sub-

TABLE V. Cross sections for Ar K photoabsorption. All cross sections are in kb (10^{-21} cm^2). σ_{tot} is obtained in each case by adding theoretical L- and M-shell contributions obtained from Ref. 14.

$E-E_{\text{trh}}$ (Ry)	E_{expt} (eV)	σ_k (c.g.)	σ_{tot}	$\sigma_K(^1P)$	σ_{tot}
0.4	3211	92.0	101.6	85.5	95.2
0.8	3216	89.0	98.6	83.3	92.9
1.2	3222	86.4	95.9	80.8	90.3
1.6	3228	84.2	93.7	79.1	88.6
2.0	3233	82.2	91.8	77.3	86.8
2.4	3238	81.2	90.8	76.4	85.8
3.0	3245	78.9	88.3		
3.5	3254	77.4	86.8	73.1	82.5
4.0	3260	76.3	85.7		
6.0	3288	72.3	81.7	68.9	78.3
8.0	3315	70.2	79.6	66.3	75.7
10.0	3342	66.5	75.9	63.9	73.3

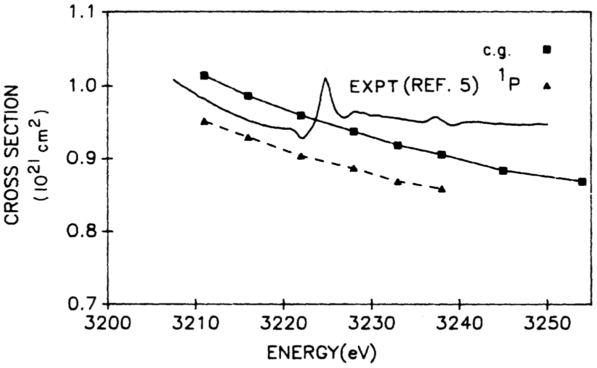

FIG. 1. Calculated and experimental cross sections.

shells, it is well known that correlation effects must be included to obtain realistic estimates of valence-shell cross sections. Since near-threshold double excitation implies excitation of a valence-shell electron, one would expect that they will be important in inner-shell double excitation processes as well. Actually, ground-state correlation provides a direct mechanism for double-electron excitation as we shall see below.

In the present context, and assuming *LS* coupling is valid, the lowest double excited configurations above the $1s3p^6$ ionization threshold will be $1s3p^54s^2$, $1s3p^54p^2$, and $1s3p^53d^2$. These configurations may be considered to be the lowest lying elements of $4sns$, $4pnp$, and $3dnd$ channels, but actually, the situation is slightly more complicated. Assuming that only ^1P states may be excited, there will be two channels corresponding to $4sns$ excitations and six each for $4pnp$ and $3dnd$ excitations. Core relaxation provides a mechanism by which the six $4pnp$ channels may be reached, owing to the nonorthogonality of the $4p$ and np orbitals with the $2p$ and $3p$ core orbitals. However, all of the channels can be reached in principle. Ground-state correlation may be considered as a mixing of the $1s^23p^6$ ground state with doubly excited configurations of the form $1s^23p^4nln'l$. When such mixing occurs, double excited states may be reached via $1s$-$3p$ excitations from the correlated ground state.

A. Ground-state correlation

In order to determine which final-state channels are most important for two-electron excitation I made several calculations of the effects of ground-state correlation using the following procedure: For configurations of the type $3p^4nln'l'$ calculations were performed in the center-of-gravity approximation and mixed with the $3p^6\,{}^1S_0$ ground state. The lowest lying state obtained by this procedure lies below the Hartree-Fock ground state, and the energy difference ΔE is a measure of the correlation energy. The calculations include not only discrete configurations such as $3p^43d^2$ and $3p^44s^2$, but also "pseudocontinuum" configurations of the type $3p^43\,d\epsilon d$ which represent a range of continuum energies above the $3p^43d$ threshold and have a width of 1 Ry. Table VI shows values of ΔE which were obtained by mixing various configurations. The table shows that most of the $3p^6$ correlation is due to excited configurations of the form $n\,dn'd$. Including all $n=n'=4$ states results in only a 7% increase in the correlation energy obtained from the single $3p^4\,3d^2$ configuration. A much larger contribution to the correlation energy is due to continuum configurations and the largest part of this is due to configurations near the $3p^43d$ threshold. These results are consistent with previous results. Cooper and Kelly[29] found that all $n\ dn'd$ configurations contribute 0.291 Ry to the $3p^6$ pair correlation energy, whereas $npn'p$ configurations contribute only 0.074 Ry.

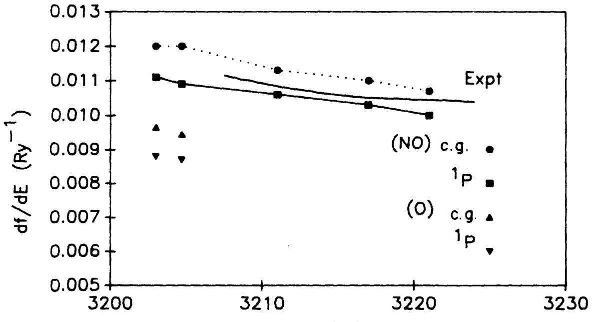

FIG. 2. Oscillator strength per unit energy.

The importance of $n\ dn'\ d$ ground-state pair correlations in outer-subshell photoionization calculations is well known,[30] and for $3p^6$ subshell photoionization, it is more convenient to use the multichannel Hartree-Fock procedure.[31] In this method, all of the correlation energy appears in terms with $nl=nl'$ and, for argon, good results can be obtained using only the $n=3$ term.

B. Resonant states above the $1s3p^6$ threshold

Center-of-gravity calculations for a number of excited configurations above the ionization threshold are shown in Table VII. Several things are apparent from these calculations. First, note the close proximity of the $3d^2$ and $4p^2$ energies and the fact that these lie only 1–2 eV below the $1s3p^53d$ threshold. The $4d^2$ and $4f^2$ configurations lie considerably above this limit, and $4s^2$ lies below it. While it is tempting to try to assign positions of resonances on the basis of calculations such as those in Table VII, as is done in Ref. 5, actually the situation is a bit more complicated. In *LS* coupling there will be three ^1P terms for each of these resonances (except for $4s^2$), and the spacing of these terms will be comparable to the energy spacings of the center-of-gravity calculations. In addition, since the terms lie so close in energy, one would expect considerable configuration mixing. Nevertheless, the calculations, along with the results shown in Table

TABLE VI. Calculations of correlation energy.

State	ΔE (Ry)
$3p^43d^2$	0.038
$3p^43d^2$+all $n=4$	0.041
$3p^43d^2+3p^43\,d\epsilon d$ ($\epsilon=0.5$)	0.185
$3p^43\,d\epsilon d(\epsilon=0.5,1.5,2.5,3.5)$	0.189

TABLE VII. Center-of-gravity calculations of doubly excited states.

State	Energy (Ry)	Energy above $1s3p^6$ (eV)
$1s3p^6$ Ar II	818.798	
$1s3p^53d$ Ar II	817.211	21.59
$1s3p^53d^2$	817.328	20.00
$1s3p^54s^2$	817.675	15.28
$1s3p^54p^2$	817.387	19.20
$1s3p^54d^2$	816.991	24.58
$1s3p^54f^2$	816.862	26.34
$1s3p^53d4d$	817.290	20.52

VI, provide an indication of why resonant structure appears immediately above the $1s3p^6$ threshold. The $3p^54p^2$ states, as well as the six $3pnp$ channels can be reached directly via core relaxation. The $3p^53d^2$ states and the $3\,dn\,d$ channels can be excited via the effects of ground-state correlation.

In order to investigate the relative magnitudes of excitation due to core relaxation and ground-state correlation, I calculated the oscillator strengths for transitions to the $1s3p^54p^2$ and $1s3p^53d^2$ configurations. The transitions to outer $4p^2$ states were calculated ignoring ground-state correlation and those to $3d^2$ outer states were made considering only mixing of the $1s^23p^6$ ground state with the $1s3p^43d^2$ configuration. The results are shown in Table VIII. Several things are apparent from these results. First, there is appreciable strength only to a single state of the $1s35^53d^2$ configuration. Second, while the strength of transitions to the $4p^2$ states is weaker, it is by no means negligible.

The above calculations lead to the following interpretation of the *KM* resonance at 19 eV above the $1s3p$ ionization threshold. The main mode of excitation is via ground-state correlation leading to excitation of the $3d^2(^3P)$ resonance. Structure above and below this resonance is due to direct excitation of states of the $4p^2$ configuration or by mixing of these states with either the $3d^2$ or higher-lying $nln'l'$ configurations.

Although a more detailed interpretation of the resonant structure would require much more detailed calculations, we can rather easily estimate the asymmetry parameters for the main resonance. The main mode of decay for the $3d^2(^3P)$ resonance will be via Auger and radiative decay of the $1s3p^5$ core, and we can estimate the width due to these processes by the 0.68-eV width obtained for the $1s3p^6$ resonance below the $1s3p^6$ ionization threshold.[27] I calculate the width of the $3d^2(^3P)$ resonance for decay to the $1s3p^6\epsilon p$ channel to be 0.025 eV, yielding a total width for the resonance of ~0.7 eV.

TABLE VIII. Positions and strengths of the $3d^2$ and $4p^2$ resonances.

State	Energy above $1s2p^6$ (eV)	Oscillator strength
$1s3p^5(^1P)3d^2(^1D)\ ^1P$	20.00	4.5×10^{-6}
$1s3p^5(^1P)3d^2(^1S)\ ^1P$	21.98	6.2×10^{-7}
$1s3p^5(^3P)3d^2(^3P)\ ^1P$	23.35	2.01×10^{-4}
$1s3p^5(^3P)4p^2(^3P)\ ^1P$	18.95	2.8×10^{-5}
$1s3p^5(^1P)4p^2(^1D)\ ^1P$	20.32	7.2×10^{-5}
$1s3p^5(^1P)4p^2(^1S)\ ^1P$	21.06	3.4×10^{-6}

The cross section for a single resonance may be represented as[15]

$$\sigma(\varepsilon)=\sigma_c\{\rho^2[(q+\varepsilon)^2/(1+\epsilon^2)]+1-\rho^2\}\ , \tag{11}$$

where $\varepsilon=2(E-E_0)/\Gamma$. Here E_0 is the resonance position, Γ the total width, q the asymmetry parameter, and ρ^2 is a measure of the fraction of the total cross section σ_c which can be reached by decay of the resonance into the same channels that can be excited by nonresonance absorption. Since the $1s$-εp channel is the main channel for absorption in the resonance region, it is a good approximation to ignore contributions to ρ and q from other channels. Thus, to first order ρ and q may be evaluated by the simple expressions:

$$q^2=2f/\pi\Gamma_f(df/dE)\ , \tag{12}$$

$$\rho^2=\Gamma_f\sigma_{1s}/\Gamma_{\sigma_c}\ , \tag{13}$$

where f is the oscillator strength of the resonance, df/dE the oscillator strength/unit energy range to the $1s$-ϵp continuum, and Γ_f the width of the resonance for decay to the $1s$-ϵp continuum. From the calculated value of $df/dE=0.105\ \text{Ry}^{-1}$ at the resonance energy and the values $f=2.01\times10^{-4}$ and $\Gamma_f=0.025\ \text{eV}=1.84\times10^{-3}$ one obtains a q^2 value of 6.62. The ratio σ_{1s}/σ_c is approximately 0.9 yielding from Eq. (13) a ρ^2 value of 0.032. These values seem to be consistent with the results of Fig. 1. For positive q, the minimum value of the cross section will lie slightly below the resonance and will be $1-\rho^2$ times σ_c, the total nonresonant cross section, consistent with the small decrease in cross section below the resonance position. The maximum value will be $\sigma_c(\rho^2q^2+1)$, and our parameter values would indicate a 20% increase in cross section at the resonance peak. The measured increase is only about 10%, which is consistent, since no attempt has been made to account for the experimental resolution of the cross section which is approximately the same as the natural linewidth of the resonance.

Quite recently, Sukhorukov *et al.*[2] reported a detailed calculation of the near-threshold double excitation cross section which agrees quite well with the experimental results of Ref. 5. In their work they included the effects of core relaxation in causing transitions to $1s3p^5nln'l'$ configurations and to the $4p\epsilon p$ and $5p\epsilon p$ channels but include no effects of initial-state correlation. It is difficult to see on the basis of the work reported here how such good agreement can be obtained ignoring ground-state correlation. My results, as well as those of Refs. 29 and 30, clearly show that most of the valence-shell correlation energy is due to $3p^4n\ dn'd'$ channels and that this correlation produces large effects of the near-threshold valence-shell cross section and 1–2% effects on the *K*-shell cross section. Their calculations also predict single-electron cross sections 5% larger than the experimental values of Ref. 5, in disagreement with the results reported here.

VI. SUMMARY AND SUGGESTIONS FOR FUTURE WORK

In the present paper I have examined in some detail the effects of core relaxation and electron correlation on the near-threshold K-shell absorption cross section. The key results are that realistic cross sections can be obtained provided core relaxation is included, thus confirming earlier work[6,8] and that both core relaxation and outer-shell electron correlation provide mechanisms for two-electron excitation. These results also point to the need for further theoretical and experimental work. On the theoretical side, there appear to be several topics requiring attention. First, if one ignores core-relaxation effects, it is possible in principle to systematically improve photoionization calculations via many-body perturbation techniques, random phase approximation methods, or by explicitly including electron-electron correlation in initial and final states. For inner-shell excitation where relaxation effects are important, further work is needed to incorporate the effects of core relaxation into these methods. Second, it appears that for argon K-shell excitation, double excitation can occur either via core relaxation or as a result of ground-state correlation. Further work is needed to determine which (if either) is the dominant mechanism. Finally, work is needed to extend this type of calculation to higher energies and make contact with the simple one-electron models that work so well far above threshold.

This work also suggests some useful experiments. Although my near-threshold calculations show good agreement with experiment, it must be remembered that the accuracy of the experimental cross sections is only of the order of 4%. Better measurements are needed to determine which of the alternative methods of calculating near-threshold single-electron cross sections yield the best results and can be used for model calculations for other elements. Finally, this work suggests some useful photoelectron spectroscopy measurements. A determination of the angular distribution of the satellite line reported by Korbin *et al.*[33] could in principle determine whether core relaxation or ground-state correlation was the most important process leading to double excitation.

ACKNOWLEDGMENTS

I would like to thank my colleagues R. Deslattes, P. Cowan, and D. Lindle for their support and encouragement during the course of the work reported here and R. Cowan for help in using the atomic structure programs.

---

[1] J. W. Cooper, in *Atomic Inner Shell Processes,* edited by B. Crasemann (Academic, New York, 1975), p. 160.

[2] E. B. Salomon and J. H. Hubbell, NBS Internal Report No. 86-3431, 1986 (unpublished).

[3] M. H. Chen, B. Crasemann, K. N. Huang, M. Aoyagi, and H. Mork, At. Data Nucl. Data Tales **19**, 97 (1977).

[4] S. I. Salem, S. C. Panosaian, and R. A. Krause, At. Data Nucl. Data Tables **14**, 91 (1974).

[5] R. D. Deslattes, R. E. LaVilla, P. E. Cowan, and A. Henins, Phys. Rev. A **27**, 923 (1983).

[6] V. L. Sukhorukov, V. V. Demekhin, V. V. Timoshevskaya, and S. V. Larventev, Opt. Spectrosk. **47**, 407 (1979) [Opt. Spectrosc. (USSR) **47**, 228 (1979)].

[7] M. Ya. Amusia, V. K. Ivanov, and V. A. Kupchenko, J. Phys. B **14**, L667 (1981).

[8] J. Tulkki and T. Aberg, J. Phys. B **18**, 1489 (1985).

[9] L. G. Parratt, Phys. Rev. **56**, 295 (1939).

[10] G. Brogren, Nova Acta Regiae Soc. Sci. Ups. **14**, No. 4 (1948).

[11] H. W. Schnopper, Phys. Rev. **131**, 2558 (1963).

[12] C. Bonnelle and F. Wuilleumier, C. R. Acad. Sci. **256**, 510 (1963).

[13] P. W. Cowan (private communication).

[14] J. H. Scofield, Phys. Rev. **179**, 9 (1969).

[15] U. Fano and J. W. Cooper, Rev. Mod. Phys. **44**, 441 (1968).

[16] R. J. W. Henry and L. Lipsky, Phys. Rev. **153**, 51 (1967).

[17] D. J. Kennedy and S. Manson, Phys. Rev. A **5**, 227 (1972).

[18] L. Lipsky and J. W. Cooper, in *Proceedings of the Fifth International Conference on the Physics of Electronic and Atomic Collisions, Leningrand, 1967,* edited by I. P. Flaks (Nanka, Leningrad, 1967).

[19] D. R. Hartree, *The Calculation of Atomic Structures* (Wiley, New York, 1957).

[20] D. R. Hartree, in Ref. 19, p. 58.

[21] P. L. Bagus, Phys. Rev. **139A**, 619 (1965).

[22] P. Lowdin, Phys. Rev. **97**, 1474 (1955).

[23] T. Aberg, Phys. Rev. **156**, 35 (1967).

[24] J. H. Scofield, Phys. Rev. A **9**, 1041 (1974).

[25] R. Cowan (unpublished); see also *The Theory of Atomic Structure and Spectra* (University of California Press, Berkley, 1981).

[26] F. Clementi and C. Roetti, At. Data and Nucl. Data Tables **14**, 177 (1974).

[27] R. D. Deslattes, Phys. Rev. **186**, 1 (1969).

[28] T. Watanabe, Phys. Rev. **139A**, 1747 (1965).

[29] E. R. Cooper, Jr. and H. P. Kelly, Phys. Rev. A **7**, 38 (1973).

[30] J. R. Swanson and L. Armstrong, Jr., Phys. Rev. A **15**, 661 (1977).

[31] C. Froese-Fisher, J. Comput. Phys. **13**, 502 (1973).

[32] V. L. Sukhorukov, A. N. Hopersky, I. D. Petrov, V. A. Yavn, and V. F. Demekhin, J. Phys. (Paris) **48**, 1677 (1987).

[33] P. H. Kobrin, S. Southworth, C. M. Truesdale, D. W. Lindle, U. Becker, and D. A. Shirley, Phys. Rev. A **29**, 194 (1984).